JOURNAL OF SOLID STATE CHEMISTRY 104, 422–436 (1993)

Synthesis and Structure of Valleriite, a Layered Metal Hydroxide/Sulfide Composite

ANTHONY E. HUGHES, GARY A. KAKOS,*
TERENCE W. TURNEY,† AND TIMOTHY B. WILLIAMS

CSIRO Division of Materials Science and Technology, Locked Bag 33, Clayton, Victoria 3168, Australia

Received April 20, 1992; in revised form November 12, 1992; accepted November 17, 1992

Optimum conditions have been determined for the hydrothermal synthesis of valleriite from mixtures of Fe/Cu sulfide and Mg/Al hydroxide gels. X-ray diffraction, electron microscopy, and X-ray photoelectron spectroscopy studies confirm a structure consisting of alternating brucite-like (Mg,Al) hydroxide layers and Cu–Fe–S sulfide layers. Energy-dispersive X-ray analysis of good quality crystals prepared from different starting ratios indicate that valleriite is stable within the composition range $[CuFeS_2] \cdot 1.67[Mg_{0.70}Al_{0.30}(OH)_2]$ to $[Cu_{1.30}Fe_{0.70}S_2] \cdot 1.35[Mg_{0.74}Al_{0.26}(OH)_2]$. A combination of XPS and EDX suggests that valleriite contains Cu^+ and mainly Fe^{3+} cations.

1. Introduction

The mineral valleriite belongs to an interesting class of crystal structures which comprise two or more misfitting and chemically dissimilar component layers. Such "noncommensurate" or "misfit" layer structures are known with an extremely diverse range of chemical compositions, from intercalated graphites though oxides, oxyfluorides, and silicates to heavy-metal sulfides and sulfosalts (*1*). The common feature of all these materials is the incommensurability of the unit meshes of the (usually two) alternating component layers, and hence there is a need for an alternative to the usual three-dimensional crystallographic description of the whole structure. One approach is to invoke separate unit cells and symmetries for each component layer and describe the overall structure in terms of these separate entities. This allows for cases where no single cell and symmetry are known, or where such a single "true-cell" is uncertain or inconveniently large, for example the mineral cannizzarite (*2*). A subset of these layered materials exists in which the component layers "match" after a small integral number of component repeats in one or both intralayer directions (2 : 3, 3 : 5, etc.), and their structures are termed "semicommensurate." Here a single "true-cell" can often be used to describe the complete structure. Other materials are known which display large but integral matches of the components in one or more directions (*3*), and others in which the layers appear to be truly incommensurable. Electron diffraction techniques have been used to good effect in studying the cell parameters and structures of these layered materials, including valleriite (*4*).

Although the component layers are mismatched (and this may extend to the layer stacking vectors, which may diverge) they are frequently joined by strong chemical bonds which arise from the residual "net charges" on the two layers. Hence, the dissimilar component structures are chemically closely interrelated. Clearly, materials

* On leave from the Chemistry and Physics Division, Institute of Education, University of Melbourne, Parkville, Victoria 3052, Australia.

† Author to whom correspondence should be addressed.

0022-4596/93 $5.00

TABLE I

REPORTED FORMULATIONS FOR VALLERIITE MINERALS

Locality	Reference	Composition
Loolekop, South Africa	(5)	$[Cu_{0.93}Fe_{1.07}S_2]1.526[Mg_{0.68}Al_{0.32}(OH)_2]$
Kaveltorp, Sweden	(6)	Range of compositions, typically $[Cu_{0.82}Fe_{1.18}S_2]1.56[Mg_{0.83}Fe_{0.17}(OH)_2]$
Noril'sk, Siberia	(7)	$[Cu_{0.99}Fe_{1.01}S_2]1.472[Fe(OH)_2]$
Palabora, South Africa	(6)	$[Cu_{1.04}Fe_{0.96}S_2]1.67[Mg_{0.75}Al_{0.09}Fe_{0.16}(OH)_2]$
Outokumpu, Finland	(8)	$[Fe_{1.26}Ni_{0.74}S_2]1.61[Mg_{0.84}Fe_{0.16}(OH)_2]$
Akagame, Japan	(9)	$[Cu_{1.13}Fe_{0.83}S_2]1.77[Mg_{0.82}Al_{0.18}(OH)_2]$
Western Australia	(10)	Range of compositions extrapolated to an ideal of $[Fe_{1.01}Cu_{0.79}S_2]1.47[Mg_{0.63}Cr_{0.37}(OH)_2]$
Talnaka, USSR	(11)	A range of compositions for various valleriites were categorized according to the predominant metals in the proposed hydroxide layer. Fe-, Mn-, Al–Mg-, Mg-, and Ca-variants were distinguished.
Silvbergsfallet, Sweden	(12)	A range of compositions: $[Cu_{0.81}Fe_{1.19}S_2]\ n[Mg_{1-y-z}Fe_yMn_z(OH)_2]$ $m[Al(OH)_3]$, $y = 0.00–1.00$, $z = 0.00–0.32$, $n = 0.74–2.08$, $m = 0.0–0.64$, $n + m = 1.23–2.08$
Ransko, Czechoslovakia	(13)	Average formula: $[Cu_{0.938}Fe_{1.062}S_2]$ $1.575[Fe_{0.289}Mg_{0.222}Cr_{0.219}Mn_{0.144}Al_{0.016}Ca_{0.100}Ti_{0.01}(OH)_2]$.

with these structures offer considerable potential for composition variations without some of the usual prerequisite of structural compatibility at the atomic level and may offer new combinations of physical and chemical properties. Little, however, is known of the general principles and conditions which govern the formation of such materials and rather less of the properties of the (usually) naturally ocurring species.

Valleriites occur in many localities, some of which are listed in Table I. The crystal structure of a South African valleriite was determined by Evans and Allmann by single-crystal X-ray diffraction methods (5). It may be described as an alternating stacking (see Fig. 1) of positively charged "brucite-like" layers of composition $[Mg_{0.68}Al_{0.32}(OH)_2]^{+0.32}$ and negatively charged "sulfide" layers of composition $[Fe_{1.07}Cu_{0.93}S_2]^{-\delta}$. The Fe and Cu atoms in the sulfide layer randomly occupy all the tetrahedral interstices between a pair of (trigonal) cubic close-packed S layers, an antifluorite XM_2 packing. A large superlattice may be used to describe the structure but as several different structural modifications of valleriite are known (1), it is more convenient to use two separate sublattices: one (rhombohedral R-3m, sublattice) with

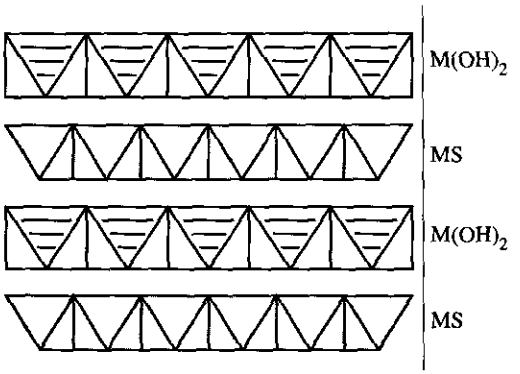

FIG. 1. Schematic drawing of the vallerite structure. Two $M(OH)_2$ layers (ruled $[M(OH)_6]$ octahedra) and two M_2S_2 layers (shaded $[MS_4]$ tetrahedra) are shown. The repeat distance between the layers in this figure, given by the intralayer matching, is five octahedra = six tetrahedra; the match is thus semicommensurate. In real valleriite the match is irrational (incommensurate). The repeat in the layer-stacking direction is one layer pair for both types here: in the reported structure (5) adjacent M_2S_2 layers are offset, giving a three-layer-pair repeat for the structure.

hexagonal axes $a = 3.79$ Å, $c = 34.10$ Å corresponding to a sulfide layers (S) and one (hexagonal, $P\text{-}3m1$) with $a = 3.07$ Å, $c = 11.37$ Å corresponding to the hydroxide layers (H). The area ratio of the two subcells in the common (intralayer) plane is given by the subcell parameters; $a_S^2/a_H^2 = (3.79)^2/(3.07)^2$ suggested the "ideal" composition of Evans and Allmann's specimen to be S : 1.52 H which was in agreement with the analytical data for this specimen provided some allowance was made for the presence of some silicate and calcium oxide impurities. The **a** and **c** vectors of both subcells are parallel. The residual charges on the two component layers are of interest: Evans and Allmann (*5*) suggested for their analyzed crystal that the net charge on the hydroxide layer, $1.52 \times (+0.32) \approx +0.49$, was balanced by an equal charge on the $[M_2S_2]$ sulfide layer, resulting from an average metal valence of about +1.76. These authors also suggested that the sulfide layer valence electrons were delocalized, leading to the metallic appearance of the mineral.

The arrangement of alternately stacking positively charged brucite-like hydroxide layers and negatively charged species is a structural feature held in common with hydrotalcites and chlorites. Materials such as these, involving ordered layer composites, are conceptually important in that they form an interface between physical mixtures and discrete chemical compounds.

The compositions of naturally occurring valleriites, according to electron microprobe elemental analyses, vary considerably; sometimes even within specific deposits. In particular, the brucite-like layers can contain a wide variety of metals in place of the Mg and/or Al in Evans and Allmann's valleriite crystal structure. An indication of the range of occurrences and compositions for these families of minerals is given in Table I. Uncertainty remains about many of the reported compositions as full single-crystal X-ray data cannot usually be obtained (*1*). Moreover, most of the reported samples contained imbedded impurities such as $Al(OH)_3$ or layer silicates, which obviously affected the compositions.

The only reported synthesis of valleriite is that of Iiishi *et al.* (*14*) who prepared some impure valleriite samples, including a chromium-substituted variety, by reacting mixtures of chalcopyrite or elemental copper, iron and sulfur with MgO and Al_2O_3 or $Cr(OH)_3$ in sealed tubes at 400–700°C and at a p_{H_2O} of 10^2 MPa. Based on the starting mixtures they gave a valleriite composition of $[CuFeS_2] \cdot x[Mg_{0.68}Al_{0.32}(OH)_2]$, $2 \leq x \leq 2.3$. Their work suggested that valleriite had an upper limit of stability at ~600°C. Later studies of the thermal behavior of valleriite from Kaveltorp, Sweden, were carried out by other workers. Harris and Vaughan (*15*) suggest that valleriite began to decompose in an inert atmosphere at 114°C, whereas DTA and TG studies coupled with X-ray powder diffraction by La Inglesia *et al.* (*16*) indicated complete decomposition in the range 450–550°C. In an oxidizing atmosphere, valleriite decomposed between 250 and 430°C. Obviously there is a good deal of uncertainty about the composition, thermal behavior, and conditions for the synthesis of valleriite. We report here the results of a hydrothermal synthetic study of these materials. Our current interest in these and related compounds is a consequence of work (*17*) on the controlled synthesis of inorganic materials with layered structures with interesting and potentially useful properties.

2. Experimental

2.1. Coprecipitation Procedure

Typically, 0.002 mole of each of Cu $(NO_3)_2 \cdot 3H_2O$ and $Fe(ClO_4)_2 \cdot 6H_2O$ were dissolved in distilled water (ca. 5 ml). This mixture was stirred with 10% w/w $(NH_4)_2S$(aq) L.R. grade (usually 10 ml, see Table II), resulting in a black suspension. A separate Mg/Al hydroxide gel was prepared by adding 25% NH_3(aq) to the desired proportion (see Table II) of $Mg(NO_3)_2 \cdot 6H_2O$ and $Al(NO_3)_3 \cdot 9H_2O$ previously dissolved in the minimum amount of distilled

TABLE II

SUMMARY OF HYDROTHERMAL EXPERIMENTS FOR VALLERIITE[a]

Expt.	Reactant stoichiometry (mmole) Cu	Fe	S	Mg	Al	Initial pH of mix.	Temp. (°C)	Heating time (days)	Phases identified by XRD
						(i) Method 1: Coprecipitation procedure			
1a	2.0	2.0	4.0	2.08	0.98	8.8	250	2	Fe_2O_3 (haematite)
1b	2.0	2.0	14.6	2.08	0.98	9.2	200	3	$CuFeS_2$
2	2.0	2.0	14.6	2.08	0.98	8.8	110	25	Valleriite
3	2.0	2.0	14.6	2.08	0.98	8.8	150	7	Valleriite, trace of $CuFeS_2$
4	2.0	2.0	14.6	2.08	0.98	8.8	150	3	Valleriite and fukuchilite
5	2.0	2.0	14.6	2.08	0.98	9.5	200	3	Valleriite, traces of FeS_2 and $CuFeS_2$
6	2.0	2.0	14.6	2.08	0.98	8.8	250	1	$CuFeS_2$ and valleriite
7	2.0	2.0	14.6	2.08	0.98	8.8	300	7	$CuFeS_2$ and some pyrrhotite
8	2.0	2.0	14.6	1.36	0.64	8.8	250	1	$CuFeS_2$
9	2.0	2.0	14.6	2.72	1.28	8.9	250	1	$CuFeS_2$ and valleriite
10	2.0	2.0	14.6	4.08	1.92	9.2	250	1	$CuFeS_2$ and trace of unidentified phase
11	2.0	2.0	14.6	5.44	2.56	9.2	250	1	$CuFeS_2$ and hydrotalcite
12	2.0	2.0	14.6	1.50	1.50	8.9	150	3	Valleriite and fukuchilite
13	2.0	2.0	14.6	1.50	1.50	9.2	200	2	Valleriite, $CuFeS_2$, traces of FeS_2 and boehmite
14	2.0	2.0	14.6	2.25	0.75	9.3	150	3	Valleriite and fukuchilite
15	2.0	2.0	14.6	2.25	0.75	9.3	200	3	Valleriite, $CuFeS_2$, FeS_2
16	2.5	1.5	14.6	2.08	0.98	9.4	200	2	Valleriite, trace FeS_2
17	2.5	1.5	14.6	1.50	1.50	9.2	200	3	Valleriite, some $CuFeS_2$, trace boehmite
18	2.5	1.5	14.6	2.25	0.75	9.4	200	3	Valleriite, some $CuFeS_2$
19	3.0	1.0	14.6	2.08	0.98	9.4	200	3	Valleriite and covellite
20	1.5	2.5	14.6	2.08	0.98	9.4	200	2	FeS_2, fukuchilite, trace valleriite
21	2.0	2.0	4.0	2.08	0.98	8.6	150	3	$CuFeS_2$
22	2.0	2.0	4.5	2.08	0.98	8.5	150	2	$CuFeS_2$
23	2.0	2.0	4.5	2.08	0.98	8.5	200	2	$CuFeS_2$, some valleriite
24	2.0	2.0	8.0	2.08	0.98	8.9	150	3	$CuFeS_2$, some fukuchilite
25	2.0	2.0	11.8	2.08	0.98	9.1	150	3	Valleriite, $CuFeS_2$ and fukuchilite
26	2.0	2.0	17.6	2.08	0.98	9.2	150	3	Valleriite and fukuchilite
27	2.0	2.0	38	2.08	0.98	9.5	150	7	Valleriite, trace of fukuchilite
						(ii) Method 2: Use of Pre-formed Hydrotalcite			
28	2.0	2.0	14.6	2.25	0.75	9.4	150	4	Valleriite and fukuchilite
29	2.0	2.0	14.6	2.25	0.75	9.4	200	4	Valleriite and $CuFeS_2$

[a] All experiments except 1a and b used hydrogen gas in the reaction mixture (see text).

water, until the pH was in the range 8.5–9.5. This hydroxide gel was then added to the sulfide suspension while stirring and the final pH recorded. An autoclave (Parr model 4740, 316 SS, 71 ml) was charged with this mixture plus a Teflon-coated stirring bead, flushed three times with hydrogen to 3 MPa, sealed at an initial partial pressure of hydrogen of 1 MPa at STP and then heated (see Table II) in a block heater positioned on a magnetic stirrer.

After the reaction period, the autoclave was cooled and any gases were vented. The product slurry was filtered under reduced pressure and the solid was washed with distilled water and then acetone to assist drying at room temperature. Table II (experiments 1–27) summarizes the experimental condi-

tions and the phases identified in the products.

2.2. *Use of Preformed Hydrotalcite*

A quantity of 0.002 mole of each of Cu $(NO_3)_2 \cdot 3H_2O$ and $Fe(ClO_4)_2 \cdot 6H_2O$ were dissolved in about 5 ml of distilled water. To this stirred aqueous mixture was added 10 ml of 10% $(NH_4)_2S$(aq), resulting in a black suspension. Then 0.003 mole of freshly calcined (450°C, 4 hr) and finely ground (120 mesh) hydrotalcite made by the method of Reichle (*18*), was added to the sulfide mixture and stirring continued for a few minutes before transferring to an autoclave as before. The experiments are summarized in Table II (experiments 28, 29).

2.3. *Analysis*

The solid products were examined by X-ray powder diffraction (XRD) using a Siemens D-500 diffractometer with Ni-filtered CuK_α radiation. Samples were prepared as air-dried suspensions on a glass plate. Wet chemical analyses were done by inductively coupled plasma atomic emission spectroscopy or by atomic absorption spectrophotometry. Selected preparations were examined by transmission electron microscopy and diffraction (TEM) together with energy-dispersive X-ray analysis (EDX) in a Philips CM30 300 kV scanning transmission electron microscope (STEM). The samples were dispersed ultrasonically in ethanol and a drop of this suspension placed on a holey carbon coated nickel grid. EDX analyses used an EDAX ultrathin window detector and EDAX software for standardless thin film quantitative analysis. The (Mg/Al) and (Cu/Fe) metal ratios in each layer were determined to reasonable accuracy by the EDX software alone, but determination of the ratio of the heavy (sulfide layer) to light (hydroxide layer) metals is complicated by the difference in energy between the Mg, Al and Fe, CuK_α groups of peaks (with SK_α lying in between, near to the Mg and Al peaks) and the resulting uncertainties in absorption, k factor, and other corrections. We therefore employed reference materials to standardize the EDX analyses. Samples of well-characterized natural chalcopyrite, $Cu_{0.97}Fe_{0.93}S_2$, and olivine, $Mg_{1.89}Fe_{0.175}SiO_4$, were kindly supplied by the South Australian Museum. A natural valleriite from the type locality of Palabora, also supplied by the South Australian Museum, was examined in order to complement the studies of the synthetic material. Only individual thin, plate-like crystals were analyzed in order to reduce absorption correction errors. Such crystals were analyzed using the scanning (STEM) mode of the CM30, usually at magnifications of $\sim 10^5$ times. In addition, transmission electron diffraction patterns and high-resolution images were made from selected samples. X-ray Photoelectron Spectroscopy (XPS) was carried out in a Vacuum Generators ESCALAB using an AlK_α X-ray source (1486.6 eV, 150 W) operated at a pressure of 10^{-9} Torr. Specimens were mounted as loose powders onto stainless steel specimen holders. Binding energies were referred to the C1*s* line at 284.6 eV.

3. Results

3.1. *Bulk Phase Analysis*

3.1.1. Physical characterization. Hydrothermal treatment of Cu/Fe/Mg/Al hydroxide/sulfide gels gave a range of products, very dependent upon reaction conditions and stoichiometry (Table II). Not only was valleriite identified, but also hematite, chalcopyrite, fukuchilite, covellite, pyrrhotite ($Fe_{1-x}S$), and pyrite (FeS_2), as well as hydrotalcite and boehmite phases. A systematic study of the yield and crystallinity of the valleriite was undertaken as a function of the experimental parameters. Although black as an aggregate, valleriite crystals have a bronze-yellow luster visible under low-power light microscopy. They dissolve slowly in cold concentrated nitric acid, but much faster in cold aqua regia.

3.1.2. The use of hydrogen in the synthe-

sis. It was found necessary to charge the autoclave with hydrogen gas to produce valleriite in the hydrothermal reaction; an initial pH_2 of about 1 MPa was sufficient for this purpose. Experiments 1a and b are two cases of reactions performed in the absence of hydrogen. The role of hydrogen in valleriite production is unclear, although its use suppressed the formation of haematite (Fe_2O_3). As discussed below, under stoichiometry requirements, the necessity for hydrogen seems to be associated with the requirement of a large excess of sulfide ions in the reaction mixture.

3.1.3. The effect of temperature and heating time. Experiments 2–7 in Table II examine the influence of reaction temperature using a reaction mixture corresponding to Evans and Allmann's (*5*) composition $CuFeS_2 \cdot 1.526\ [Mg_{0.68}Al_{0.32}(OH_2)]$ but with excess sulfide. When temperatures in excess of 250°C were employed, valleriite was not observed in the XRD patterns of the products. A temperature of 110°C coupled with a long heating time (experiment 2) led to the sample with the highest purity and crystallinity, based on XRD. At temperatures between 150 and 200°C other Cu–Fe–S phases were observed in the XRD of the products, such as chalcopyrite and fukuchilite. It is possible that under these conditions a chemical equilibrium between valleriite and fukuchilite and/or chalcopyrite exists. In any case, our results are not consistent with Iiishi *et al.*'s (*14*) observation of valleriite phases up to 600°C, nor with the results of La Inglesia *et al.*'s (*16*) DTA and TG study.

The results of our thermal study are summarized in a schematic phase diagram shown in Fig. 2. Fukuchilite was not observed in the products of reactions carried out at temperatures above 200°C, consistent with the relative thermal stabilities for fukuchilite and chalcopyrite (*19*). The observation of pyrrhotite in the products of reactions carried out at 300°C is also in accord (*20*) with the relative thermal stabilities of chalcopyrite and pyrrhotite. Experiments 3 and 4 indicate that the heating time influenced the products of the hydrothermal reactions. At 150°C, after 3 days, both fukuchilite and chalcopyrite were observed as products in addition to valleriite, but if the heating time was increased, fukuchilite formation appeared to be less favorable.

3.1.4. The [Cu + Fe]/[Mg + Al] ratio. Experiments (6, 8–11) in Table II show that the mixing ratio [Cu + Fe]/[Mg + Al] is also important for the formation of valleriite. Valleriite was only observed in the products of reactions where this mixing ratio was of the order of 1 ~ 1.3. Lower ratios led to the formation of chalcopyrite and hydrotalcite, while a ratio of 2 produced only chalcopyrite. The use of an excess of Mg^{2+}-rich hydroxide component in the reaction mixture (experiment 11) led to the formation of a Mg, Al–hydrotalcite derivative (*21*), where, instead of the Cu–Fe–S layer, probably sulfide and/or nitrate ions and H_2O occupy the region between the hydroxide layers.

3.1.5. Variation of the amount of sulfide in the reaction mixture. Experiments 21–27 in Table II examine the critical effect of the amount of sulfide on the products of reaction mixtures with Cu : Fe = 1 : 1 and Mg : Al = 0.68 : 0.32 and T = 150 ~ 200°C. The results of this study are incorporated in Fig. 2. Unless both hydrogen and an excess of sulfide over that required by the formula $CuFeS_2$ were employed in the reaction mixture, valleriite was not observed among the products. As shown in Table II, experiments 21, 22, 24, and 25 carried out at 150°C suggest that of the order of 200% excess sulfide was needed to form valleriite at this temperature. At 200°C (exp. 23), a smaller excess was required. As the degree of excess sulfide (experiments 26, 27) and the time of heating increased, the proportion of valleriite in the products increased. The reason for the requirement of excess sulfide ion in conjunction with hydrogen for the formation of valleriite is unclear. Its significance is not suggested by the crystal structure of valleriite (*5*), with an excess of sulfide not evident in the elemental analyses of the products.

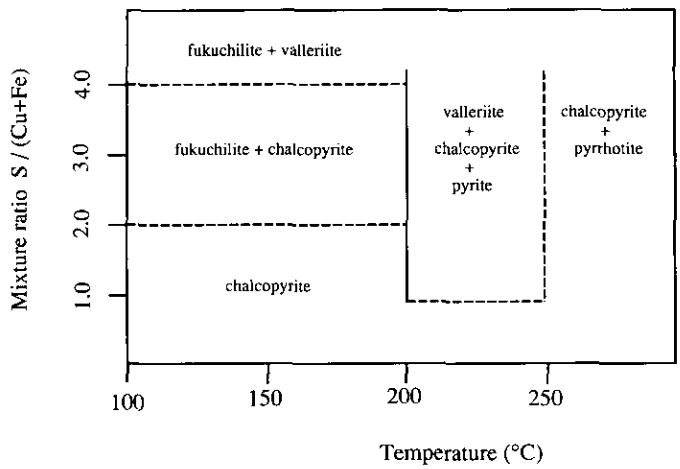

FIG. 2. Schematic nonequilibrium phase diagram summarizing our hydrothermal syntheses of valleriite and other compounds. Lines bounding the different phase regions were not determined accurately and are given as guides only.

3.1.6. The Cu/Fe and Mg/Al ratios. Experiments 16–20 in Table II summarize the reaction products obtained at 200°C when the reaction ratio Cu^{2+}/Fe^{2+} was varied from 0.60 to 3.00, while that of Mg^{2+}/Al^{3+} was varied from 1.00 to 3.00, keeping the amount of sulfide constant. It appears that there is some flexibility in the Mg/Al ratio in the formation of valleriite and this is confirmed by the EDX elemental analyses discussed below. A significantly higher Cu^{2+}/Fe^{2+} ratio in the reaction mixture (experiments 16, 17, 18 in Table II) seemed to favor the formation of valleriite, whereas a higher proportion of Fe^{2+} (experiment 20) favored the formation of pyrite. Moreover, the mixtures with a higher proportion of Cu^{2+} resulted in improved crystallinity of the valleriite products, judging from the sharpness of the XRD peaks. In the case of the Mg/Al ratio, as this approached equimolar, a significant amount of boehmite was observed among the products.

3.1.7. Reaction of Cu^{2+} + Fe^{2+} + S^{2-} with calcined (Mg, Al)-hydrotalcite. Thermal decomposition of preformed hydrotalcite, $[Mg_6Al_2(OH)_{16}][CO_3 \cdot xH_2O]$, at 450–500°C has been shown to form a poorly crystallized phase capable of taking up a wide variety of anions, such as chromate, permanganate and sulfate ions (*22*) and polyoxometallate ions (*23*) to form crystalline layered phases in which the new anion is incorporated into the interlayer region, resulting in substantial increases in the basal spacing. The reaction of calcined hydrotalcite with Cu^{2+}–Fe^{2+}–S^{2-} mixtures was briefly examined in the hope of finding a more convenient method of producing purer, better crystallized samples of valleriite than that produced by the coprecipitation method. Valleriite was indeed produced in reactions carried out at 150°C and 200°C (see Table II, experiments 28, 29), with the proportion of valleriite in the products increasing with temperature. However, the 150°C and 200°C products contained significant amounts of fukuchilite and chalcopyrite respectively.

3.2. X-Ray Diffraction

The XRD *d* spacings and intensities for the product of experiment 2, our most crystalline sample, are listed in Table III and compared to those published (JCPDS #29-554) for a mineral specimen of Valleriite

TABLE III

COMPARISON OF X-RAY POWDER DIFFRACTION DATA FOR SYNTHETIC AND NATURALLY OCCURRING (Mg,Al)-VALLERIITES

Loolekop specimen (JCPDS #29-554)		Synthesis by Iishi *et al.* (*14*)		This work[a]		
d	*I*	*d*	*I*	*d*	*I*	*h k l*[b]
11.41	100	11.40	60	11.0	60	0 0 3
5.71	100	5.72	100	5.52	100	0 0 6
3.80	50	3.81	15	3.70 (br)	15	0 0 9
3.27	60	3.27	20	3.24 (br asym)	40}	1 0 1
					}	0 1 2
3.07	20			3.04 (br)	20	1 0 4
2.958	10					0 1 5
2.846	50			2.79 (br)	10	0 0 12
2.604	10					0 1 8
2.364	20					1 0 10
2.259	20	2.265	5			0 1 11
2.041	20	2.049	5			1 0 13
1.885	50	1.893	10		}	0 0 18
1.860	50	1.871	10	1.87 (v.br)	25}	1 1 3
					}	
1.780	10					1 0 16
1.629	10					0 0 21
1.526	10					2 0 8

Note. br = broad peak, asym = asymmetrical peak, v.br = very broad peak. Intensities normalized to most intense peak = 100.

[a] Product from Experiment 2 (see Table II).

[b] Hexagonal crystal system, $a = b \neq c$, $\alpha = \beta = 90°$, $\gamma = 120°$.

from Loolekop, South Africa and to those from the sample synthesized by Iiishi *et al.* (*14*). The powder pattern confirms the hydrothermal synthesis of valleriite. The peaks can be indexed with an hexagonal unit cell of dimensions $a = 3.78 \pm 0.01$ Å, $c = 33.5$ Å $\pm$ 0.1 Å, corresponding to the sulfide sublattice in the crystal structure of Evans and Allmann (*5*). However, the c parameter is significantly smaller than those reported for both the Loolekop specimen (34.1 Å) and the synthetic material of Iiishi *et al.* (34.18 ~ 34.44 Å) (*14*). Also, all the peaks are fairly broad, indicating considerable disorder. The reflections from the hydroxide layer were not observed in the XRD patterns. There appeared to be no significant change in the XRD *d* spacings as the Cu/Fe and Mg/Al ratios were varied in the syntheses.

3.3. Electron Microscopy, EDX, and XPS Studies

3.3.1. HRTEM and electron diffraction. The extremely small crystallite size and low crystallinity of the bulk of most preparations presented considerable problems in obtaining structural information. As Fig. 3 shows, the valleriite preparations usually comprised masses of plate-like "nanocrystallites" of various sizes and in a variety of orientations, and in many cases it was very difficult to select "single" crystals for either EDX or diffraction studies. Deformed, needle-like or fibrous crystallites were also present. Although some platelets were of the order of 1 μm in size (Fig. 4), they were often associated with unidentifiable material and in most cases, analyses were done on smaller fragments, perhaps 0.1 ~ 0.05 μm. Furthermore, although we could find quite

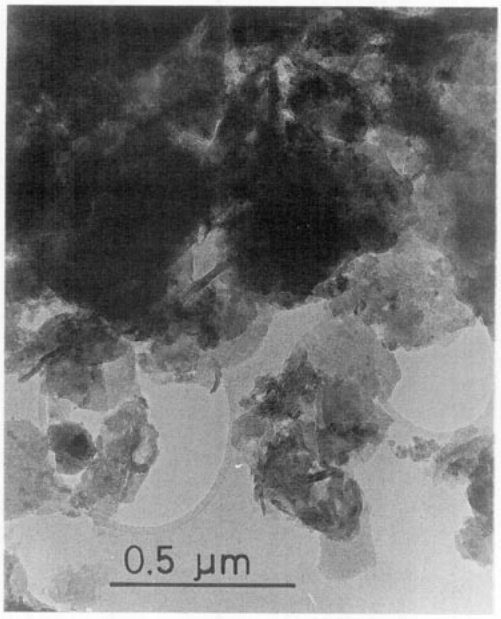

FIG. 3. Low magnification TEM image of material from preparation 3 showing the massed plate-like and short needle-like material typical of all valleriite-containing preparations.

well-formed "hexagonal" crystallites in some preparations (experiments 2, 3, 16), frequently these proved to be chalcopyrite. Where we were certain, from EDX analysis and electron diffraction, that we were examining "valleriite" crystals, the thin, often hexagonally shaped platelets were at best only partially crystallized (evidenced by the poor lattice-fringe contrast and ring-diffraction patterns from single plates). In many platelets, we could not obtain clear diffraction from both substructures, as the $M(OH)_2$ layer diffraction was often extremely diffuse. However, with care we could obtain good diffraction patterns from a sufficiently large number of platelets to confirm the two independent hexagonal sublattices reported for valleriites (Fig. 5a). The diffraction intensity from the sulfide layer was usually in the form of a sharp, spotted ring (Fig. 5b,c), indicating a layer consisting of well-ordered "islands" in many orientations, essentially a turbostratic structure. Although often diffuse, the hydroxide layer reflections were usually present as six spots, indicating better long-range orientational order than the sulfide substructure. In contrast with many other layered, "incommensurate" materials no intralayer "true-cell" seems to exist: the crystallinity appears to be present over too short a distance for the formation of such a long-period modulated structure. Hence, only reflections from the substructures were observed. A very common [001] zone-axis pattern is shown in Fig. 5b. A sharp ring of diffraction intensity corresponding to the sulfide layer 110 reflections indicates a well formed, albeit "nanocrystalline" layer: locally there are many different orientations with a common **c** direction. The hydroxide layer 110 reflections are diffuse and somewhat distorted, although the range of orientations is much more restricted. Figure 5c shows another type of disorder, also observed in the natural sample: a (100) ring for the sulfide layer is accompanied by two sets

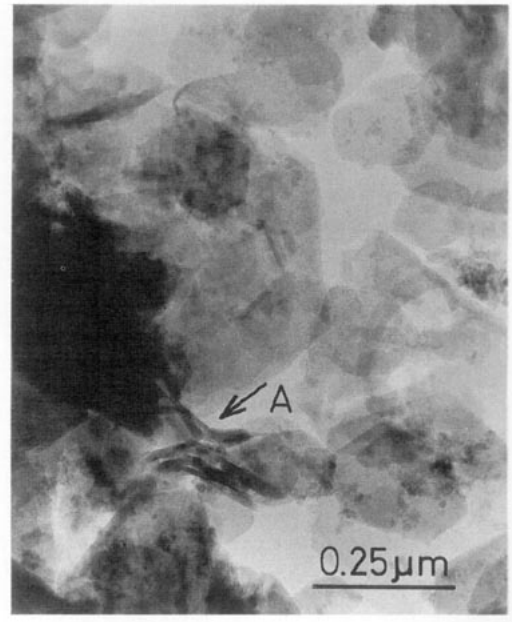

FIG. 4. TEM image from preparation 2, a sample which was nearly pure valleriite. Thin, platy valleriite crystals compose the bulk of this sample. The region arrowed "A" is enlarged in Fig. 6a.

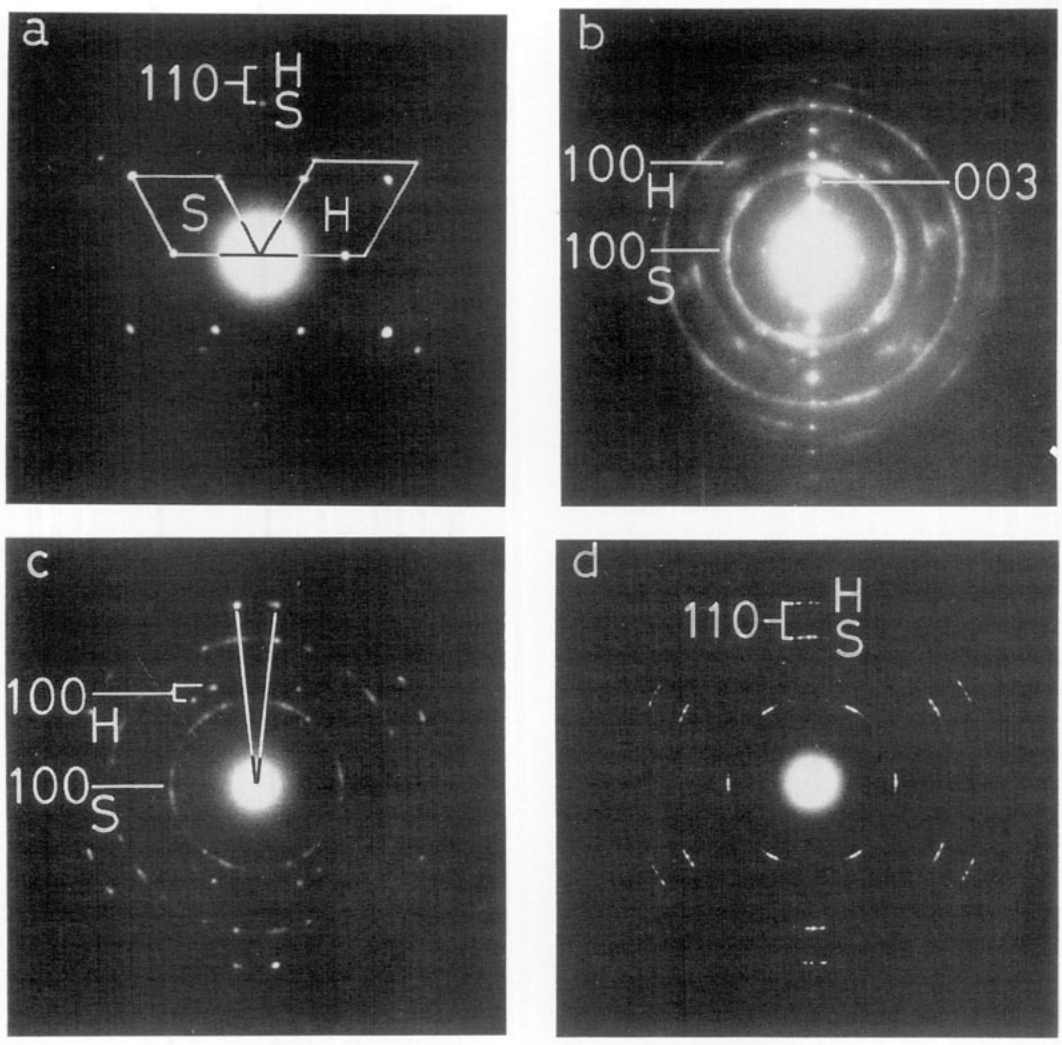

FIG. 5. Selected-area diffraction patterns of different valleriite crystals from preparation 2. (a) A "perfect" plate-like crystal showing two independent hexagonal reciprocal sublattices, S and H, from the sulfide and hydroxide layers respectively. (b) Pattern from a region containing a well-ordered crystal "edge-on" (needle-like material in the images) which shows reflections from a valleriite layer-spacing of ~11 Å. Rings of 100 type indicate somewhat disordered or nanocrystalline plate-like material in this region. (c) From a plate-like crystal showing a fairly common type of disorder, with two "twin" orientations of the well-ordered hydroxide layer and a ring of sulfide reflections indicating nanocrystallinity. The hydroxide twinning angle is ~13°. (d) A crystal with both layers disordered by rotation through various angles about [001], although most nanocrystals are within about ±5° from each other.

of rather sharp hydroxide layer spots, rotated by about 13° with respect to each other. Several other crystals were also found which gave approximately this 13° rotation and also a disordered form (Fig. 5d).

Figure 6 shows images from needle-like crystallites, which could also be narrow pieces of platelet viewed edge-on. Such images showed quite clear fringes with a spacing of about 11 Å, corresponding to the valleriite *d* (001). These needles were usually highly distorted and were extremely

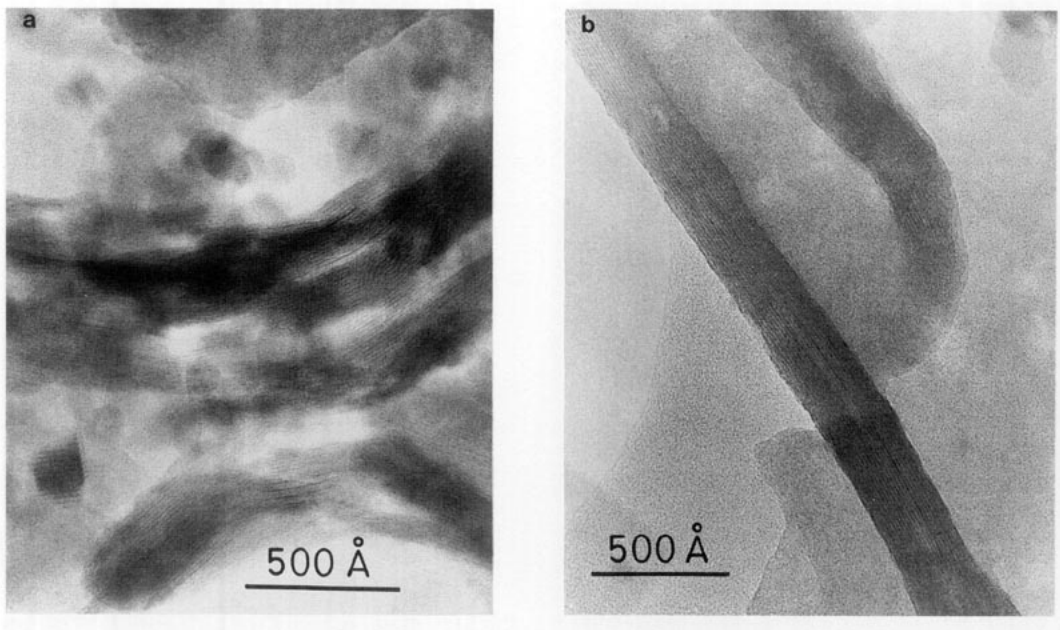

FIG. 6. TEM images from the needle-like material of preparation 2, showing the structural homogeneity of the synthetic valleriite. (a) shows broken fragments and fine-scale distortions of the fragile plates.

thin (typically only 150 Å thick), and often bent over very small radii. The images and corresponding diffraction patterns (Fig. 5b) show only a repeat of ~11 Å: there is no diffraction evidence for longer range stacking order such as the three-layer, 34 Å c parameter reported for the sulfide layer in Ref. [5]. In some images, individual layers showing a markedly darker fringe contrast were seen, perhaps indicative of some compositional differences (Fig. 6b). However, it is clear from Fig. 6 that the materials prepared contain regions which are well ordered and are not predominantly physical mixtures of separate metal sulfide and hydroxide phases on a nanometre scale.

In the majority of the valleriite samples examined by TEM, chalcopyrite could be detected although the amount varied considerably from sample to sample. Except in the preparations containing well-crystallized valleriite, the larger parts of the TEM samples consisted of agglomerates of material which could not be identified from the diffraction data, being finely polycrystalline or "amorphous," and which had widely varying compositions, doubtless influenced in part by absorption problems caused by the thickness of some such agglomerates. Use of the analytical data must therefore be made with due consideration for this unidentified material.

Our analyses of the reference materials olivine and chalcopyrite suggested that the Fe/Mg ratios obtained from the EDX analyses were sufficiently accurate to be used without further normalization. The Cu/Fe and the S/(Cu + Fe) ratios were corrected after the reference samples were analyzed. Since only well-formed, individual platelets were selected for analysis, it is likely that our analyses are somewhat biased towards those conditions which favor the formation of "large" platelets. In the case of experiments 5, 13, 15, and 20, the poor crystallinity of the product and thus the difficulty in finding "good" material for analysis severely reduced the number of analyses which were obtained.

3.3.2. EDX vs reaction mixture cation ra-

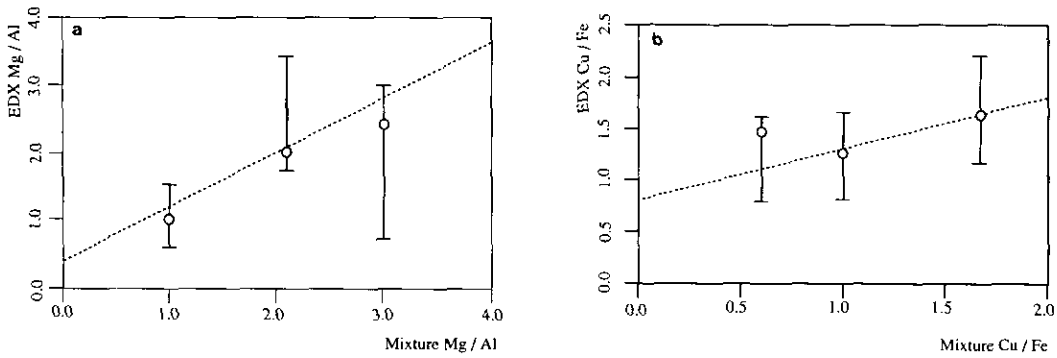

FIG. 7. Summary of the correlation between our starting and EDX analyzed cation ratios for valleriite, showing (a) Mg/Al and (b) Cu/Fe ratios. The EDX data were obtained from good quality single crystals and are presented as average analyses (open circles) and bars giving the range of values in the data set. The dotted line is a least-squares fit as a guide to the eye. Correlation between the starting and the final compositions was much closer in the hydroxide layer than in the sulfide layer.

tios. Both the Cu/Fe and Al/Mg ratios were varied in the syntheses and it was of particular interest whether these variations were reflected in the compositions of the product valleriites. Figure 7 summarizes these results: there is a reasonable correlation between the mixed and observed Mg/Al ratios, which varied over the approximate range 1.0 ~ 2.5. On the other hand, for those samples sufficiently crystalline to examine, the observed Cu/Fe ratio remains close to 1.5 despite variation in the starting composition between 0.6 and 1.67.

3.3.3. XPS analysis of metal oxidation states. The XPS binding energies obtained from measurements on samples from experiments 2 and 16 are presented in Table IV. For comparison the binding energies for chalcopyrite are also included since the oxidation states for Cu and Fe are known to be I and III respectively (*24*). Cu $2p_{3/2}$ and Cu (*KLL*) are both presented since it is well known that a combination of both must be used to distinguish the Cu(0) and Cu(I) oxidation states by XPS (*25*). It can be seen in Fig. 8 that the Cu data for chalcopyrite and experiments 2 and 16 all fall within the Cu(I) region, establishing that Cu(I) is the only form of copper present in the samples.

The Fe oxidation states are more difficult to determine due to partial surface oxidation giving rise to Fe(III) in an oxidized form, probably associated with sulfate, which was detected in the *S* 2*p* spectra. Similar surface oxidation was observed for the chalcopyrite and is difficult to avoid for air-exposed mixed Cu–Fe sulfides (*26*). Consequently, curve fitting was employed to extract the components arising from the sulfide and other species. There were clearly two components in the Fe $2p_{3/2}$ spectra; a low binding energy component related to the pure sulfide and a high binding energy component arising from the oxidized species. The binding energies and percentage of the total intensity (figures in brackets) of both components are presented in Table IV. The low binding energy component in both experiments 2 and 16 had similar values to the Fe(III) binding energy in chalcopyrite, suggesting the presence of Fe(III) in both samples. Carver *et al.* (*27*) have established that XPS binding energies increase with the charge on the atom. Hence the shift by 0.5 eV to lower binding energy of the Fe $2p_{3/2}$ peak for experiment 2, although nearly at the level of experimental error, may well reflect a lower charge on the sulfide Fe atoms.

3.3.4. Metal oxidation states in the sulfide

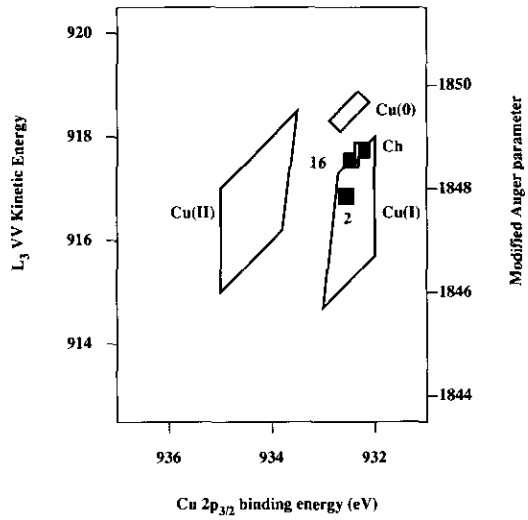

FIG. 8. Summary of the Cu XPS measurements from samples 2 and 16 given in Table IV. The L_3VV kinetic energy and modified Auger parameter are plotted as a function of the Cu $2p_{3/2}$ binding energy. Filled squares indicate the experimentally determined values for samples from experiments 2 and 16 and pure chalcopyrite. All lie in the Cu(I) region of the diagram. For reference, the Cu(II) and metallic Cu (0) regions are also shown.

layer from EDX analyses. The ratio of S/(Cu + Fe) was determined after the analyses were corrected with the chalcopyrite standard, and the average over all the valleriite crystals examined was close to unity (0.95), with a few individual analyses varying between about 0.55 and 1.27. For the most extensively analyzed sample (experiment 16; Cu/Fe = 1.67, Mg/Al = 2.0), from which ten analyses of plate-like valleriite crystals were obtained, the Cu/Fe ratio was 1.53 from the EDX analyses, suggesting a composition for the sulfide layer of $[Cu_{1.20}Fe_{0.80}S_2]$. Since the hydroxide layer metal oxidation states are known, we can determine the values for the sulfide layer from the Mg/Al and interlayer $[M_2S_2]/[M'(OH)_2]$ cation ratios, provided that the hydroxide layer is assumed to be stoichiometric. The $[M_2S_2]/[M'(OH)_2]$ ratio can be

TABLE IV

XPS BINDING ENERGIES[a]

	Experiment 2	Experiment 16	$CuFeS_2$
Cu $2p_{3/2}$	932.6	932.5	932.6
Cu (*KLL*)	916.9	917.5	917.6
Fe $2p_{3/2}$	707.5(11)[b] 710.5(89)[c]	708.0(20)[b] 711.1(80)[c]	708.1(33)[b] 709.4(67)[c]
Al $2p$	75.1	75.6	—
O $1s$	530.1 532.3[d]	532.6[d]	—
S $2p$	162.5(69)[b] 169.1(31)[c]	162.4(68)[b] 169.6(32)[c]	161.4[b]

[a] All binding energies were referred to the C $1s$ line at 284.6 eV ± 0.2 eV error. Numbers in brackets represent relative intensities.

[b] Iron sulfide S^2-transition.

[c] Iron sulfate $[SO_4]^2$-transition.

[d] Sulfate oxygen.

TABLE V

ELEMENTAL COMPOSITION OF SYNTHETIC VALLERIITES[a]

Expt. no.	Number of analyses	Composition	Average Fe oxid. state
16	10	$[Cu_{1.20}Fe_{0.80}S_2].1.57[Mg_{0.70}Al_{0.30}(OH)_2]$	+2.9
2	9	$[Cu_{1.04}Fe_{0.96}S_2].1.67[Mg_{0.70}Al_{0.30}(OH)_2]$	+2.6
3	7	$[Cu_{1.10}Fe_{0.90}S_2].1.83[Mg_{0.70}Al_{0.30}(OH)_2]$	+2.6
18	3	$[Cu_{1.28}Fe_{0.72}S_2].1.35[Mg_{0.74}Al_{0.26}(OH)_2]$	+3.3

[a] Determined by EDX analyses on a number of individual thin crystals within each preparation.

determined independently from both EDX analyses and in principle from the electron diffraction patterns, if on the latter a pair of corresponding, intralayer sulfide and hydroxide lattice spacings can be measured. For this sample, which had an EDX Mg/Al ratio of 2.30 (starting mixture 2.10) and EDX interlayer ratio $[M_2S_2]/[M'(OH)_2]$ of 1 : 1.57, we have a net charge on the hydroxide layer of +0.3 per $[M'(OH)_2]$ formula unit, which must be balanced by 0.64 $[M_2S_2]$ units, giving a net charge of −0.47 per sulfide formula unit $[M_2S_2]$. This suggests a composition $[Cu_{1.20}Fe_{0.80}S_2] \cdot 1.57[Mg_{0.70}Al_{0.30}(OH)_2]$. Clearly, the presence of Cu^{2+} and Fe^{2+} are excluded by this argument as the average metal oxidation state is +1.76, but a reasonable charge balance is obtained by assuming Cu^+ and $Fe^{2.9+}$ for this sample. The final composition of plate-like valleriite samples with different starting compositions (experiments 2 and 3 Cu/Fe = 1.0, Mg/Al = 2.0 and experiment 18 Cu/Fe = 1.67, Mg/Al = 3.0) were calculated similarly from an average of the analyses on individual crystallites. The results, shown in Table V, highlight the considerable compositional flexibility encompassed by the valleriite structure.

4. Conclusions

We show that valleriites with a range of compositions can be synthesized hydrothermally, and that nearly single-phase products are formed under certain reaction conditions. Although the products are nanocrystalline, and as such present difficulties to their study by X-ray methods, TEM combined with high-resolution EDX analysis in the microscope has proven invaluable in examining these materials. Albeit within a small range, changes in the reaction mixture are reflected in the composition of well-formed product crystallites, indicating that the valleriite structure is able to accommodate some variation in the individual layer compositions, although we found little evidence for variation in the alternating layer sequence. Although not unequivocal, analysis of EDX and XPS spectra from these valleriites strongly suggests that copper is predominantly present as Cu^+, while iron is mainly Fe^{3+}, as has been found with chalcopyrite (*24*).

Acknowledgments

The authors are grateful to Dr. A. Pring, South Australian Museum, for providing the mineral samples used in this study. We are also indebted to P. Miller (NAMAC), P. R. Curtis, and M. Fergus for technical assistance.

References

1. E. MAKOVICKY AND B. G. HYDE *Mater. Sci. Forum* **100/101,** 1 (1992).
2. E. MATZAT, *Acta Crystallogr. Sect. B* **35,** 133 (1979).
3. T. B. WILLIAMS AND A. PRING, *Am. Mineral.* **73,** 1426 (1988).
4. N. I. ORGANOVA, V. A. DRITS, AND A. L. DMITRIK, *Am. Mineral* **59,** 190 (1974).
5. H. T. EVANS AND R. ALLMAN, *Z. Kristallogr.* **127,** 73 (1968).

6. G. SPRINGER, *Neues Jahrb. Mineral. Monatsh.* **8,** 252 (1968).
7. D. C. HARRIS, L. J. CABRI, AND J. M. STEWART, *Am. Mineral.* **55**(2), 10 (1970).
8. M. HUHMA *et al., Bull. Geol. Soc. Finland* **45,** 103 (1973).
9. Y. MURAMATSU, N. NAMBU, AND T. TAKEUCHI, *J. Jpn. Assoc. Mineral. Petrol. Econ. Geol.* **70,** 236 (1975).
10. E. H. NICKEL AND D. R. HUDSON, *Contrib. Mineral. Petrol.* **55,** 265 (1976).
11. L. N. EMELINA *et al., Zap. Vses. Mineral O-Va.* **111,** 84 (1982).
12. I. S. OEN, I. SCHMIERMANN, AND W. J. LUSTENHOUWER, *Neues. Jahrb. Mineral. Monatsh.*, **5,** 209 (1985).
13. Z. JOHAN, *Neues. Jahrb. Mineral. Monatsh.*, **6,** 269 (1990).
14. K. IISHI, T. TOMISAKA, T. KATO, AND S. TAKENO, *Am. Mineral.* **55,** 2107 (1970).
15. D. C. HARRIS AND D. J. VAUGHAN, *Am. Mineral.* **57,** 1037 (1972).
16. A. LA INGLESIA, M. DOVAL, AND F. LOPEZ-AGUAYO, *Am. Mineral.* **62,** 1030 (1977).
17. (a) L. A. BRUCE, J. V. SANDERS, AND T. W. TURNEY, *Clays Clay Miner.* **34,** 25 (1986); (b) S. HARDIN, D. HAY, M. MILLIKAN, J. V. SANDERS, AND T. W. TURNEY, *Chem. Mater.* **3,** 977 (1991).
18. W. T. REICHLE, *J. Catal.* **94,** 547 (1985).
19. J. R. CRAIG AND S. D. SCOTT, *in* "Reviews in Mineralogy" (P. H. Ribbe, Ed.), vol. 1, Chap. 5, p. CS-65, Mineralogical Society of America (1976).
20. J. R. CRAIG AND S. D. SCOTT, *in* "Reviews in Mineralogy" (P. H. Ribbe, Ed.), Vol. 1, Chap. 5, p. CS-25, Mineralogical Society of America, 1976.
21. W. T. REICHLE, *Solid State Ionics* **22,** 135 (1986).
22. T. SATO, T. WAKABAYASHI, AND M. SHIMADA, *Ind. Eng. Chem. Prod. Res. Dev.* **25,** 89 (1986).
23. K. CHIBWE AND W. JONES, *Chem. Mater.* **1,** 489 (1989).
24. I. NAKAI, Y. SUGITANI, I. NAGUSHIMEA, AND Y. NIWA, *J. Inorg. Nucl. Chem.* **40,** 789 (1978).
25. M. A. KOHLER, H. E. CURRY-HYDE, A. E. HUGHES, B. A. SEXTON, AND N. W. CANT, *J. Catal.* **108,** 323 (1987).
26. D. BRION, *Appl. Surf. Sci.* **5,** 133 (1980).
27. J. C. CARVER, K. SCHWEITZER, AND T. A. CARLSON, *J. Chem. Phys.* **57,** 973 (1972).